Periodic coherence-peak height modulations in superconducting $Bi_2Sr_2CaCu_2O_{8+\delta}$

A. Fang,[1] C. Howald,[2] N. Kaneko,[3,*] M. Greven,[1,3] and A. Kapitulnik[1,2]

[1]*Department of Applied Physics, Stanford University, Stanford, California 94305, USA*

[2]*Department of Physics, Stanford University, Stanford, California 94305, USA*

[3]*Stanford Synchrotron Radiation Laboratory, Stanford, California 94309, USA*

In this paper we analyze, using scanning tunneling spectroscopy (STS), the local density of electronic states (LDOS) in nearly optimally doped $Bi_2Sr_2CaCu_2O_{8+\delta}$ in zero magnetic field. We see both dispersive and nondispersive spatial LDOS modulations as a function of energy in our samples. Moreover, a spatial map of the superconducting coherence peak heights shows the same structure as the low-energy LDOS. This suggests that these nondispersive LDOS modulations originate from an underlying charge-density modulation, which interacts with superconductivity.

I. INTRODUCTION

The scanning tunneling microscope (STM) has been an important tool in the study of high-temperature superconductors since their discovery. Initially, a variety of gap sizes and structures were found and introduced much controversy into the subject. Later, a more coherent consensus among different groups emerged regarding the surface properties of these high-T_c materials. To give a few examples, STM studies revealed the nature of the superstructure in $Bi_2Sr_2CaCu_2O_{8+\delta}$ (BSCCO),[1] the d-wave nature of the gap and its size,[2] the effect of local impurities, the emergence of zero-bias anomalies,[3–5] and the electronic structure of the core of vortices.[6,7] More recent measurements suggest that superconductivity may not be homogeneous in high-T_c superconductors. In particular, STM measurements have found spatial variations of the gap size in YBCO[8] and BSCCO.[9–11]

While gap inhomogeneities have been found to dominate the electronic structure at large measured bias, more ordered structures underlying the d-wavelike tunneling spectra have been found at lower energies. A current topic of great interest in high-T_c superconductors is the presence of spatial modulations of the charge and spin densities. Theoretical[12–19] and experimental[20–27] evidence has been mounting in support of the possibility that their ground state exhibits spin- and charge-density waves (SDW and CDW), which may be primarily one-dimensional (i.e., stripes), or two-dimensional[28] with a characteristic wave vector in the Cu-O bond direction of $q_{\pi-0}=0.25(2\pi/a_0)$. In STM measurements such a modulation was first seen by Hoffman *et al.*[29] in a magnetic field as a 2D checkboard pattern of LDOS, aligned with the Cu-O bonds, around vortex cores in slightly overdoped BSCCO with Ni impurities. The reported modulations showed a checkerboard ordering vector of $q_{\pi-0} \approx 0.23(2\pi/a_0)$ extending to large distances when measured at bias energy ~ 7 mV. Howald *et al.*[30] shortly afterward reported this same effect in zero field on similarly doped BSCCO crystals without intentional substitution impurities. The observed modulation with ordering wave vector $q_{\pi-0} =[0.25\pm0.03](2\pi/a_0)$ was found at all energies, exhibiting features characteristic of a two-dimensional system of line

objects. Moreover, Howald *et al.* showed that the LDOS modulation manifests itself, for both a positive and negative bias, as a shift of states from above to below the superconducting gap. The fact that a single energy scale (i.e., the gap) appears for both superconductivity and these modulations suggests that these two effects are closely related.

In subsequent studies at zero field, Hoffman *et al.*[31] and McElroy *et al.*[32] measured the dispersion of the strongest Fourier peak along the $\pi-0$ (i.e., Cu-O) direction. They asserted that it was consistent with what is expected from quasiparticle scattering interference,[33] in which a peak in the Fourier LDOS equals the momentum transfer wave vector of the incident and scattered waves. In general, their data showed good agreement with photoemission results (i.e., band structure results[34]) at large bias, but did not continue to disperse below ~ 15 mV.

To account for *all* the available data in the full energy range, Vojta,[35] Podolsky *et al.*,[36] and Kivelson *et al.*[37] have shown that *both* a nondispersive or weakly dispersive charge order and strongly dispersive quasiparticle scattering effects can occur at the same time in the presence of pinned fluctuating stripes. In particular, Podolsky *et al.*, using explicit calculations, showed that for a system with incipient charge order the dispersion *for this particular effect* is very weak and less than expected by band structure. At low energy it converges to the ordering vector rather than the vector corresponding to the nodal separation on the Fermi surface. A similar conclusion was reached by Kivelson *et al.* who emphasized that at higher energies, for a relatively clean material, quasiparticle scattering interference will show a strong signal that overwhelms the weak charge modulation. At low energies, the minimum energy required to overcome the finite superconducting gap means that only quasiparticles near the nodes participate and thus should give a wave vector for the interference, which is larger than what was measured. The discrepancy was taken as evidence that another phenomenon dominates at low energies.

In this paper, we present new data and analysis on this phenomenon, measured on near optimally doped samples. Using the same apparatus with the same experimental conditions as before, we show data for two of our samples (from the same growth run): one that has a (fixed) two-dimensional

214514-1

ordering wave vector $q_{\pi-0}=[0.25\pm0.03](2\pi/a_0)$ that dominates the dispersive signal over much of the energy range,[30] and one that has a stronger dispersive signal, which begins to dominate from lower energies on up, yet still has a majority of spectral weight for the lowest energies at wave vector $q_{\pi-0}=[0.22\pm0.03](2\pi/a_0)$. We further show that for all the samples studied, the density of states at the gap (i.e., dI/dV at $V=\Delta$) exhibits modulations with a wave vector similar to the low-energy pattern. Finally, we present evidence for the interplay of these modulations and superconductivity by showing the strong supression of the large-gap coherence peaks.

II. EXPERIMENT

We performed measurements using a homemade cryogenic STM. The STM measures differential conductance $G \equiv dI/dV$, which is proportional to the LDOS. The samples are near optimally doped (slightly overdoped) single crystal $Bi_2Sr_2CaCu_2O_{8+\delta}$ ($T_c\sim86-87$ K) (Ref. 38) grown by a floating-zone method. They are cleaved at room temperature in an ultrahigh vacuum of better than 1×10^{-9} Torr, revealing an atomically flat surface between the BiO planes. Then they are quickly lowered to the cryogenic section at a temperature of $6-8$ K, where cryopumping yields orders-of-magnitude better vacuum. Typical data were taken with a sample bias of -200 mV and a set point current of -100 pA, which establishes the relatively arbitrary normalization for the LDOS. We also performed measurements with a sample bias of $+65$ mV and a setpoint current of $+25$ pA.

At each point on the surface, a spectrum (dI/dV versus sample voltage V) was taken. The bias modulation for the spectra is 1 mV$_{rms}$. This, in addition to the time constant of the lock-in amplifier used to record dI/dV, yields a total blurring of the spectra of ~3 mV. Although there are discrepancies when trying to fit a spectrum with a d-wave function, using the voltage (i.e., position) of the coherence peak maximum for the gap value Δ yields a reasonable fit and is the method we will use throughout this paper. The coherence peak-heights map is made by evaluating dI/dV at $V=\Delta$ [as shown in Fig. 1(c)]. All maps have been constructed for positive sample voltage, as this yields a better signal to noise. This observation is most likely related to the asymmetry of the conductance spectra, which are common to all BSCCO STM studies.[39]

III. RESULTS AND ANALYSIS

A. Spatial variation

Spatial variations of the superconducting gap on the surface of BSCCO have been reported by several groups, and their existence is now an established fact.[10,11,40] Typically the size of the gap varies on a length scale of roughly 30 Å as was described in detail by Howald *et al.*[10] The gaps vary from small-gap regions of ~30 mV to large-gap regions of ~60 mV. The large-gap regions usually develop from an average gap background with the largest gap at their center.[10] Figure 1(a) shows the size of the gap mapped over a typical surface. Patches about 30 Å across of varying gap size are
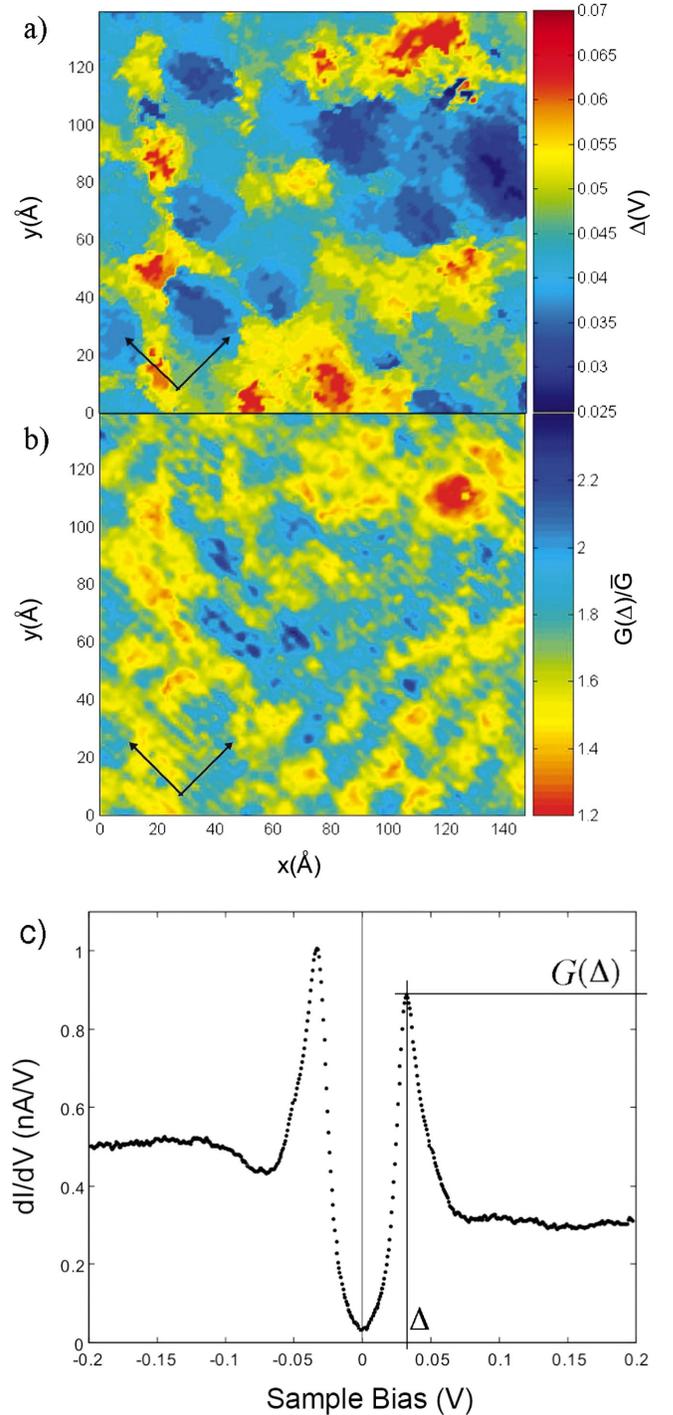
FIG. 1. (Color) (a) Gap size Δ over a 140 Å $\times$ 140 Å area. (b) Coherence peak height (divided by the average conductance) with inverted color scale. Scan performed at $+65$ mV bias. Arrows indicate direction of Cu-O bonds. Topographic supermodulation (not shown) is $45°$ to the arrows. (c) Typical BSCCO spectrum with definitions of Δ and $G(\Delta)$.

clearly visible. The distribution of gap sizes in this view is depicted in Fig. 2(a), where the average gap is $\bar{\Delta}=45.4$ mV. The smallest scale features reflect some variation with atomic resolution. In addition, the partial, nearly vertical lines show that there is some correlation between superstructure and the gap [Fig. 1(a)].
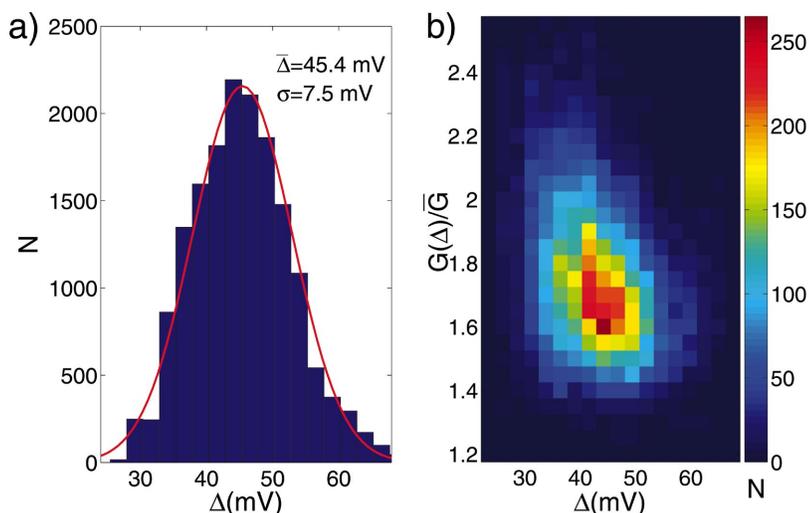
FIG. 2. (Color) (a) Histogram of gap-size distribution for the data in Fig. 1(a). (b) Density plot of coherence peak height vs gap size.

An important feature of the gap-size distribution is that the height of the coherence peaks is varying as well. There is some correlation between these two effects: those spectra with the smallest gaps typically have taller coherence peaks. This anticorrelation is depicted in Fig. 2(b), which shows the variation of the gap size and the coherence peak height for the area in Fig. 1. The color scale of Fig. 1(b) is inverted in order to demonstrate the anticorrelation shown in Fig. 2(b) (e.g., regions with large gaps tend to have shorter coherence peaks).

While there is a correlation between gap size and coherence peak height, it is not a simple one-to-one relationship. Thus the two maps can differ significantly. Aside from some high-frequency noise, the spatial variation in the peak height [Fig. 1(b)] is smoother, with no abrupt transitions between the regions. Next, we note the presence of an atomic corrugation that is stronger in one direction. This is most likely due to a convolution with the tip shape, as this effect shows up in the topographic image as well. More importantly, it is clear that the peak height shows an ordered structure (see, e.g., the lower-right corner of the figure) in which the modulation amplitude can be as great as ~30% of the mean peak height in some areas.

By inspection of spectra from −200 mV to +200 mV, we found that normalization by the setpoint current at +65 mV makes the peak-height map least sensitive to contributions from the superstructure as well as most of the low k-vector structure (which is due to gap-size inhomogeneities). Additionally, choosing a positive normalization voltage makes the spectra less dependent on the normal-state background, which is typically stronger on the negative bias side of the gap.[39] Thus taking the scan at +65 mV bias largely removes these features, as compared to a peak height map taken with a more common setpoint voltage of −200 mV. This simple procedure allows the peak height structure to be seen in the real space image. A map of the current at +65 mV for a spectroscopic scan taken at −200 mV shows little to no spectral weight above the noise near $q=0.25(2\pi/a_0)$, and, thus, this procedure would not create the modulations we see.

B. LDOS modulations, dispersion, and $G(\Delta)$

To look for LDOS modulations, one typically looks at the differential conductance $G \equiv dI/dV$ as a function of voltage

(V) at each point on the sample. In most cases modulations are more visible in Fourier space where the length scales of various features are better separated. Figure 3 shows a Fourier transform of the differential conductance of the area shown in Fig. 1 for two different energies (10 mV and 29 mV) as well as for the gap, Δ (note that the majority of gaps are 30 mV $\leqslant \Delta \leqslant$ 60 mV for that region). Circles are placed at $(2\pi/a_0)(\pm 0.25,0)$ and $(2\pi/a_0)(0,\pm 0.25)$ as reference points.

As in previous results[30] (Fig. 4), for low energies we see periodic density of state modulations at a periodicity close to $4a_0$. The periodicity (as shown by the Fourier analysis) is $(0.22\pm 0.03)(2\pi/a_0)$ for the data in Fig. 3. At low energies ($\leqslant 15$ mV), these modulations dominate [Fig. 3(a)], but as one goes up in energy, the strength of the overall signal increases and moves to longer wavelengths in a very similar way to the results of McElroy *et al.*[32] This behavior is clearly seen in Fig. 3(b) where we show a Fourier transform for a sample bias of 29 mV. (The color scale on the Fourier maps has been adjusted to keep this signal within view.) At higher energies, above ~35 mV, the signal is lost in the noise due to the appearance of coherence peaks that vary with position on the sample. Although our experimental k-resolution limits precise quantitative statements we can make about any dispersion, it is clear that overall, more spectral weight is appearing at lower k-vectors as the energy increases.

To show this dispersive effect, we take line scans along the $\pi - 0$ and $0 - \pi$ directions in Fourier space [Figs. 3(d) and 4(d)]. (Both directions give similar results, so we only show one.) At each point along the line, we weight the neighboring Fourier points with a Gaussian filter of FWHM 1.6 pixels (which is not necessarily centered directly over a pixel). The values are then squared, summed, and a square root is taken. Finally, this value is normalized by the proximity of the line to the various Fourier points. The values reported in the line scans are the total modulation amplitude in that region of Fourier space. Due to pixelation effects and the size of our scans, the uncertainty in the peak positions, as well as our resolution, is $\Delta q=0.03(2\pi/a_0)$. However, the normalization procedure and large filter width ensure that all of the features (i.e., peaks) seen are distinct and not due to pixelation artifacts (e.g., a broad peak will not be split into two by passing the line scan between pixels).
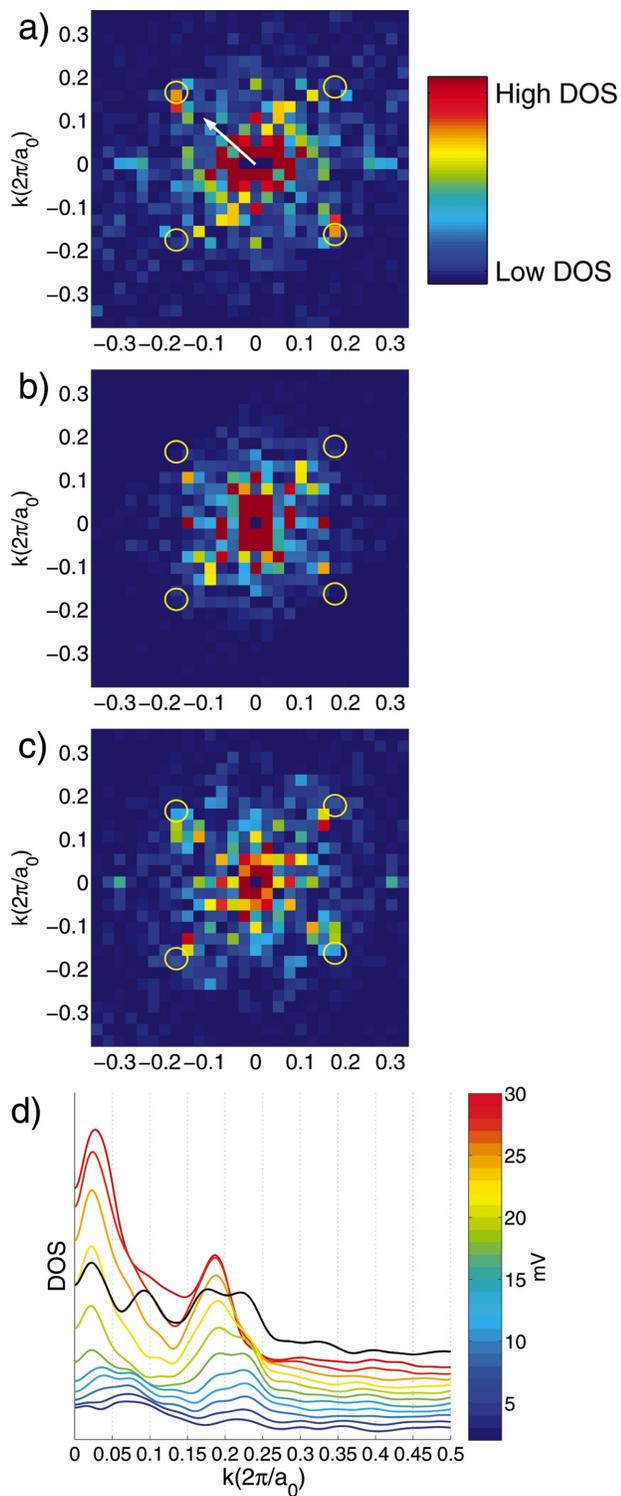
FIG. 3. (Color) (a) FFT of LDOS (dI/dV) at 10 mV. White arrow indicates direction of line scan. Circles placed at $4a_0$. (b) FFT of LDOS at 29 mV. (c) FFT of LDOS taken at the coherence peak maxima. (d) Line scans as a function of energy showing the dispersion relation of the charge modulation periodicity. Black line is for the coherence peak maxima. All lines shifted for clarity.
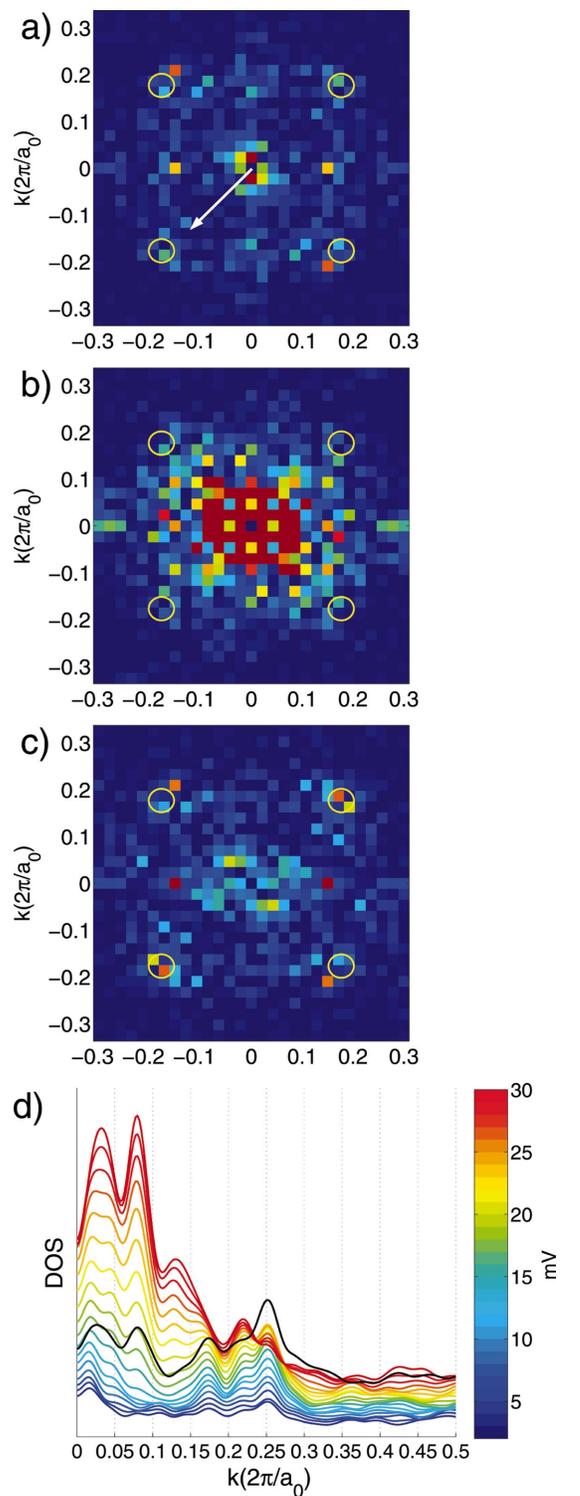
FIG. 4. (Color) From previously published dataset. (a) FFT of LDOS at 11 mV. (b) FFT of LDOS at 28 mV. (c) FFT of LDOS taken at the coherence peak maxima with additional 65 mV normalization procedure (see Sec. III C). (d) Line scans as a function of energy. Black line is for the normalized coherence peak maxima.

We observe that at all the energies shown, a (sometimes weak) signal always exists near the four-period wave vector, in agreement with Howald *et al.*[30] Additionally, there exists a signal at a slightly lower *k*-vector. This is most likely the dispersive quasiparticle scattering interference peak since it becomes suppressed upon an integration over energy, as shown for example in Fig. 9 of the above work.[30] If one follows the "main peak" as suggested by Hoffman *et al.* (i.e., using a single peak to fit both features), then dispersion is inferred at energies above ~ 15 mV. Other features also show up at lower *k*-vectors, such as $q \sim [0.08, 0.13, 0.17] \times (2\pi/a_0)$. The first two match features in a line scan of the Fourier transform of the gap-size map (i.e., spatial variations in the gap size cause a change in the DOS via a widening or narrowing of the spectra). The third may be a harmonic of $q \sim 0.08(2\pi/a_0)$.

If we consider the modulations in the peak heights [Fig. 1(b)] in Fourier space [Figs. 3(c) and 3(d), black line], we find that it is very similar to the low-energy modulation [Fig. 3(a)]. The peak-heights map has a periodic structure close to four lattice spacings [more precisely $q_{\pi-0} = (0.22 \pm 0.03) \times (2\pi/a_0)$] even though the entire contribution comes from energies above ~ 30 mV [see Fig. 2(a)]. By looking at the LDOS based on gap size, we are sampling from a range of energies whose spectra contribute in such a way as to give a modulation at a higher *q* than would be predicted by quasiparticle scattering for any of these energies alone. The peak [or shoulder in the case of Fig. 4(d)] at slightly lower *q* is likely to be from these quasiparticles at higher energies.

Finally, we note that to maximize the amplitude of the peaks, our line scan in Fig. 3(d) is rotated by $\sim 4°$ with respect to the atomic positions. This is not surprising considering that our scan size is only over a few correlation lengths, and, thus, defects can cause an overall rotation in the modulations.

C. Interaction with superconductivity

Some other interesting effects can also be seen when one compares the maps of the coherence peak heights and the gap size. Here we show a previously published dataset[30] that has been taken over a larger area (Fig. 5). An additional procedure we use here is to normalize (i.e., divide) the individual spectra by the current at +65 mV. (More precisely, we divide by the average conductance from 0 to 65 mV.) This is similar to scanning over the area with this setpoint voltage of 65 mV (as in our previous figures). We note that this procedure is only used to "clean up" the image so that certain features can be clearly seen in both real and Fourier space [note the lack of low-frequency noise in Fig. 4(c)]. As mentioned earlier, this procedure does not add any artificial modulations.

By comparing Figs. 5(a) and 5(b) [or Figs. 1(a) and 1(b)], one can see that the amplitude of the coherence peak DOS modulations tends to be larger in the regions of large gap. In contrast, regions of small gap show modulations of reduced amplitude. Since there are only a few modulation crests and troughs within a particular region of large or small gap, this effect is difficult to quantify. It can most easily be seen by
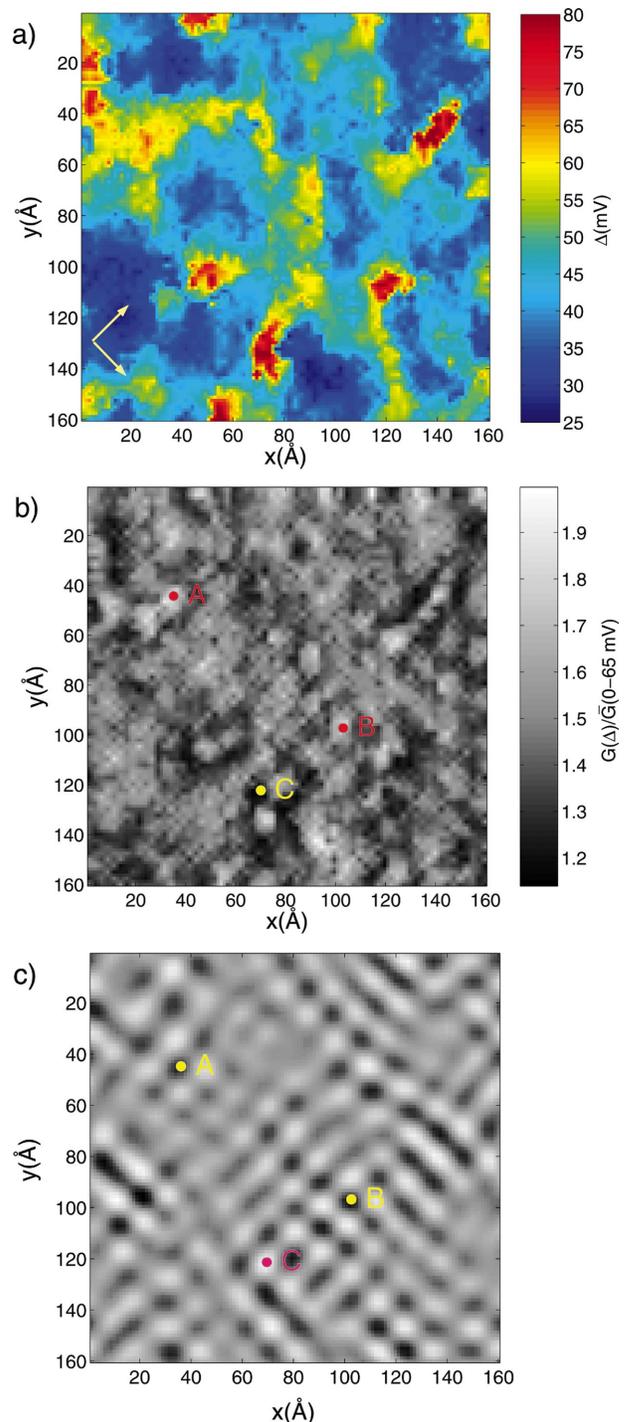
FIG. 5. (Color) (a) Gap-size distribution over a 160 Å $\times$ 160 Å area. Arrows indicate direction of Cu-O bonds. (b) Coherence peak heights, normalized. (c) LDOS at 8 mV, unnormalized, Fourier filtered. Equivalent points on Figs. (b) and (c) are marked by points A, B, and C.

noting that regions where the contrast is highest (point C, for example) correspond to large-gap regions. We note that the large amplitude modulations are not simply due to the normalization procedure (large-gap regions are renormalized to have higher LDOS due to the incomplete integration of the

coherence peaks), since they are actually a larger fraction of the mean coherence peak height.

Figure 5(c) shows the real-space LDOS at 8 mV, after Fourier filtering near the $(2\pi/a_0)(\pm 0.25, 0)$ and $(2\pi/a_0) \times (0, \pm 0.25)$ points in reciprocal space. We chose an energy where the signal from the underlying order dominates over the quasiparticle scattering interference signal. The filter is shaped like a circle, with a radius of 4 pixels in which no Fourier weight is suppressed. The edges then taper off like a Gaussian with a width of one pixel. This filter encompasses the vast majority of the spectral weight in the region and thus does not favor one particular wave vector. The filtered image shows a dominant four-period modulation that is almost checkerboardlike, but with dislocations in the form of extra half rows. By following the modulations, one can see a general correspondence between the peaks of Fig. 5(b) and the troughs of Fig. 5(c) and vice versa. The points marked A, B, and C are examples of this out-of-phase relation. (The features may not match up exactly because of noise or the slight contribution from quasiparticle scattering.) This suggests that where the low-energy modulations have an increased LDOS, the coherence peaks are suppressed and vice versa. In particular, this suppression is stronger for the large-gap coherence peaks.

IV. DISCUSSION

It has been argued before that the competition between kinetic energy and Coulomb repulsion may lead to various forms of charge- and spin-ordered states. In particular, "stripes" have been predicted to occur in doped antiferromagnets.[12,13,41,42] The discovery[43–45] of stripe order in $La_{2-x}Sr_xNiO_{4+\delta}$ and soon after in $La_{1.6-x}Nd_{0.4}Sr_xCuO_4$[46] added considerable credibility to the suggestion that stripe states form an important bridge between the Mott insulator and the more metallic state, which becomes Fermi-liquidlike at heavy doping. The theory is that at low doping, static stripes characterize a true broken symmetry state. However, upon increased doping the periodicity of the stripes decreases and coupling occurs. This is roughly the region where superconducting order wins over stripe order. Stripes will now exist in the superconducting phase in a dynamical sense, i.e., stripe order is fluctuating. Therefore no broken symmetry is expected and, thus, to preserve the point symmetry of the underlying crystal, a fluctuating checkerboard is expected. STM, however, is a static probe and thus cannot detect any structure associated with fluctuating order unless something pins it.[3–7,11,29,30,40,47] Indeed, the gap-size inhomogeneities discussed above and other forms of chemical disorder[48] are a natural source for pinning and can make stripes or checkerboards visible to STM in the form of LDOS modulations.

Fourfold symmetrical order may also be a consequence of strong interactions on the square lattice. When reduced to the low-energy Plaquette Boson Fermion Model, the system shows a checkerboard structure due to the tendency of this model to locally prefer a four-boson (an antiferromagnon triplet and a d-wave hole pair) state (i.e. doping of 1/8).[28,49] In either of the above theories, this underlying order has a

nondispersive or weakly dispersive nature. In the case of "striped" structures, weak dispersion is expected because of the finite size of the stripe domains and the interaction with the itinerant quasiparticles.[36,37]

While the above two examples result in an (almost) "fixed-q" order (i.e., a true frozen charge density visible in the LDOS at all energies at an almost constant wave vector), the existence of quasiparticles (in the broad sense)[37] in the presence of weak disorder may also add quasiparticle scattering interference effects.[33,50] In this case, quasiparticles of given energy scatter off an impurity. The resulting interference between the original and scattered waves leads to variations of the local density of states at wave vectors $\mathbf{q} = \mathbf{k} - \mathbf{k}'$, where $\mathbf{k}$ and $\mathbf{k}'$ are the wave vectors of states with energy $E = \epsilon(\mathbf{k}) = \epsilon(\mathbf{k}')$, as determined by the band structure, $\epsilon(\mathbf{k})$. Judging from measured band structure on BSCCO via photoemission,[34] quasiparticle scattering interference effects should be strongly dispersive, as is indeed seen in STM experiments for energies greater than ~15 mV.

However, analysis of all recent experiments[37] indicates that both evidence for a fixed-q oscillation[30] and quasiparticle scattering interference[31,32] have been found experimentally. Taking this point of view, it is clear that if there is an underlying order coexisting with the quasiparticle interference structure, then one needs a way to separate out these effects. The main problem here is that the large contribution of the gap inhomogeneities and the strong dispersion of the quasiparticle scattering interference cover up this underlying order. Following the ideas of Kivelson *et al.*[37] Howald *et al.*[30] showed that integration of the Fourier space LDOS over a wide range of energies reduces the influence of any random or dispersing features while at the same time enhances features that do not disperse. Another possibility is to look for the interaction of these features with another order parameter, such as superconductivity. We claim that the periodic structure observed in the LDOS at the gap, $G(\Delta)$ in Fig. 1(b), is exactly this effect.

What we see is a return of features from the low-energy region (where saturation is observed in the plot of dispersion), suggesting that these features indeed exist and are related to superconductivity. In addition, the large amplitude of these coherence peak modulations and the distinct peak near $q = 0.22(2\pi/a_0)$, as shown in the line scan of the Fourier transform of the coherence peak heights [Figs. 3(d) and 4(d)], is suggestive of some kind of coherent contribution from a nondispersive feature. (Dispersive contributions would cause a peak in the line scan to be broadened or suppressed, e.g., the peak/shoulder at lower k-vector.)

Our Fourier analysis from low energies up to the smallest gap sizes (where the noise from inhomogeneities overwhelms our signal) supports the picture presented earlier of a nondispersive or weakly dispersive feature near $q = 0.22(2\pi/a_0)$ in addition to a dispersive feature at a lower k-vector. It is likely that disorder plays a strong role in determining the relative strengths of these two signals and accounts for the differences between our samples. We find that the large amplitude of the lower k-vector feature swamps out the nondispersive feature at higher energies, but becomes weaker as one goes down in energy, until at approximately 15 mV the nondispersive signal dominates, thus explaining

the saturation. The additional line scan for the Fourier transform of coherence peak heights can be seen as a way to remove the effects of gap-size inhomogeneities to reveal that a structure at $q \approx 0.22(2\pi/a_0)$ still exists at higher energies. It makes a similar point as the spatial maps of the coherence peaks, namely, that by selectively sampling from the (higher) energies related to superconductivity, the low-energy features reappear.

Finally, we note the correspondence of these (coherence peak-height) modulations to the superconductivity as determined by the size of the gap. First, we observe that the modulation structure that resides in the regions of larger gaps is the most pronounced. These large-gap regions with low coherence peaks generally resemble slightly underdoped samples.[10] On the other hand, the modulation is suppressed and the coherence peak heights are more uniform in small-gap regions and tall coherence peaks. Gaps in these regions are more similar to gaps found in overdoped samples;[51] this is consistent with the notion that beyond optimal doping, a more homogeneous charge density exists as the system tends more toward a Fermi-liquid state.

Such an observation does not necessarily point out a competition between charge-density modulation and superconductivity, but rather reinforces the idea that the two effects coexist at and below optimal doping. One possible interpretation is that the fluctuating stripe/checkerboard phase exists in all the regions below optimal doping, and, as one moves further into overdoping (i.e., into regions of small gap), the modulations become diminished. Our observations, therefore, complement those of Vershinin *et al.*[52] who found similar patterns in the pseudogap regime of slightly underdoped $Bi_2Sr_2CaCu_2O_{8+\delta}$. As noted by Kivelson *et al.*,[37] the effect of quasiparticle scattering interference should disappear at temperatures above T_c, revealing the underlying order. For our measurements at low temperature, in regions of very large gap with weak coherence peaks (similar to the pseudogap), charge ordering is indeed visible. The two results, therefore, suggest that in the absence or suppression of superconductivity, charge ordering may be the preferred phase.

However, these "pseudogaplike" regions are only about two superconducting coherence-lengths large, while the modulations [as seen in Fig. 5(c)] persist over approximately seven periods,[29,30] suggesting that these modulations are more apparent in, but not exclusive to, these regions. Moreover, both the modulation and superconductivity seem to coexist at low temperatures for all gap sizes except that in the small-gap regions, the peak-height modulation amplitude is suppressed as discussed above. However, since the pseudogap is likely not a true phase transition, and, in terms of both doping and temperature, the system may be relatively far from a charge ordering critical point, ordering may be tenuous. Upon lowering the temperature, the system undergoes a true phase transition into the superconducting phase where one expects the fixed-wavelength modulation phenomenon to be strongly pinned in the presence of disorder. We see this effect as a nondispersive signal that additionally manifests itself in the coherence peak heights of the tunneling spectra.

V. CONCLUSION

The observation of spatial modulations in a quantity that is related to the pair amplitude, i.e., the coherence peak heights, points to the intimate relation between superconductivity and the charge modulation. This is strong evidence that the underlying modulation at $q \approx 0.22(2\pi/a_0)$, which exists down to low energies, yet reappears at gap energies, is a separate effect from the quasiparticle scattering interference signal. Further analysis of the energy dependence suggests that the "saturation" seen in plots of dispersion can be explained by the dominance of this nondispersive signal at low energies. Finally, the observation that these modulations suppress the coherence peaks most strongly in large-gap regions is consistent with a phase diagram that has an ordered phase toward underdoping and tends toward a more homogeneous charge distribution with increased doping.

ACKNOWLEDGMENTS

*Present address: National Institute of Advanced Industrial Science and Technology, Tsukuba Central 2-2, Tsukuba, Ibaraki 305-8568, Japan.

[1] M. D. Kirk, J. Nogami, A. A. Baski, D. B. Mitzi, A. Kapitulnik, T. H. Geballe, and C. F. Quate, Science **242**, 1673 (1988).

[2] C. Renner, O. Fischer, A. D. Kent, D. B. Mitzi, and A. Kapitulnik, Physica B **194**, 1689 (1994).

[3] Ali Yazdani, C. M. Howald, C. P. Lutz, A. Kapitulnik, and D. M. Eigler, Phys. Rev. Lett. **83**, 176 (1999).

[4] E. W. Hudson, S. H. Pan, A. K. Gupta, K. W. Ng, and J. C. Davis, Science **285**, 88 (1999).

[5] S. H. Pan, E. W. Hudson, K. M. Lang, H. Eisaki, S. Uchida, and J. C. Davis, Nature (London) **403**, 746 (2000).

[6] Ch. Renner, B. Revaz, K. Kadowaki, I. Maggio-Aprile, and O. Fischer, Phys. Rev. Lett. **80**, 3606 (1998).

[7] S. H. Pan, E. W. Hudson, A. K. Gupta, K.-W. Ng, H. Eisaki, S. Uchida, and J. C. Davis, Phys. Rev. Lett. **85**, 1536 (2000).

[8] H. L. Edwards, D. J. Derro, A. L. Barr, J. T. Markert, and A. L. de Lozanne, Phys. Rev. Lett. **75**, 1387 (1995).

[9] T. Cren, D. Roditchev, W. Sacks, J. Klein, J.-B. Moussy, C. Deville-Cavellin, and M. Lagues, Phys. Rev. Lett. **84**, 147 (2000).

[10] C. Howald, P. Fournier, and A. Kapitulnik, Phys. Rev. B **64**, 100504 (2001).

[11] K. M. Lang, V. Madhavan, J. E. Hoffman, E. W. Hudson, H. Eisaki, S. Uchida, and J. C. Davis, Nature (London) **415**, 412 (2002).

[12] J. Zaanen and O. Gunnarsson, Phys. Rev. B **40**, 7391 (1989).

[13] V. J. Emery, S. A. Kivelson, and H. Q. Lin, Phys. Rev. Lett. **64**, 475 (1990).

[14] V. J. Emery and S. A. Kivelson, Physica C **209**, 597 (1993); S. A. Kivelson and V. J. Emery, in *Strongly Correlated Electronic Materials*, Proceedings of the Los Alamos Symposium, 1993, edited by K. S. Bedell, Z. Wang, D. E. Meltzer, A. V. Balatsky, and E. Abrahams (Addison-Wesley, Reading MA, 1994) p. 619.

[15] A. Polkovnikov, S. Sachdev, M. Vojta, and E. Demler, in *Physical Phenomena at High Magnetic Fields IV, Oct. 19-25 , 2001, Santa Fe, New Mexico* [Int. J. Mod. Phys. B16, 3156 (2002)].

[16] J. Zaanen and A. M. Oles, Ann. Phys. (San Diego) **5**, 224 (1996).

[17] S. R. White and D. J. Scalapino, Phys. Rev. Lett. **81**, 3227 (1998).

[18] K. Machida, Physica C **158**, 192 (1989).

[19] M. Kato, K. Machida, H. Nakanishi, and M. Fujita, J. Phys. Soc. Jpn. **59**, 1047 (1990).

[20] J. M. Tranquada, J. D. Axe, N. Ichikawa, A. R. Moodenbaugh, Y. Nakamura, and S. Uchida, Phys. Rev. Lett. **78**, 338 (1997).

[21] B. Lake, G. Aeppli, K. N. Clausen, D. F. McMorrow, K. Lefmann, N. E. Hussey, N. Mangkorntong, M. Nohara, H. Takagi, T. E. Mason, and A. Schroder, Science **291**, 1759 (2001).

[22] B. Lake, H. M. Ronnow, N. B. Christensen, G. Aeppli, K. Lefmann, D. F. McMorrow, P. Vorderwisch, P. Smeibidl, N. Mangkorntong, T. Sasagawa, M. Nohara, H. Takagi, and T. E. Mason, Nature (London) **415**, 299 (2002).

[23] Y. S. Lee, R. J. Birgeneau, M. A. Kastner, Y. Endoh, S. Wakimoto, K. Yamada, R. W. Erwin, S. H. Lee, and G. Shirane, Phys. Rev. B **60**, 3643 (1999).

[24] V. F. Mitrović, E. E. Sigmund, M. Eschrig, H. N. Bachman, W. P. Halperin, A. P. Reyes, P. Kuhns, and W. G. Moulton, Nature (London) **413**, 501 (2001).

[25] B. Khaykovich, Y. S. Lee, R. Erwin, S.-H. Lee, S. Wakimoto, K. J. Thomas, M. A. Kastner, and R. J. Birgeneau, Phys. Rev. B **66**, 014528 (2002).

[26] X. J. Zhou, T. Yoshida, S. A. Kellar, P. V. Bogdanov, E. D. Lu, A. Lanzara, M. Nakamura, T. Noda, T. Kakeshita, H. Eisaki, S. Uchida, A. Fujimori, Z. Hussain, and Z.-X. Shen, Phys. Rev. Lett. **86**, 5578 (2001).

[27] K. Yamada, C. H. Lee, K. Kurahashi, J. Wada, S. Wakimoto, S. Ueki, H. Kimura, Y. Endoh, S. Hosoya, G. Shirane, R. J. Birgeneau, M. Greven, M. A. Kastner, and Y. J. Kim, Phys. Rev. B **57**, 6165 (1998).

[28] E. Altman and A. Auerbach, Phys. Rev. B **65**, 104508 (2002).

[29] J. E. Hoffman, E. W. Hudson, K. M. Lang, V. Madhavan, H. Eisaki, S. Uchida, and J. C. Davis, Science **295**, 466 (2002).

[30] C. Howald, H. Eisaki, N. Kaneko, M. Greven, and A. Kapitulnik, Phys. Rev. B **67**, 014533 (2003).

[31] J. E. Hoffman, K. McElroy, D.-H. Lee, K. M. Lang, H. Eisaki, S. Uchida, and J. C. Davis, Science **297**, 1148 (2002).

[32] K. McElroy, R. W. Simmonds, J. E. Hoffman, D.-H. Lee, J. Orenstein, H. Eisaki, S. Uchida, and J. C. Davis, Nature (London) **422**, 592 (2003).

[33] Q. H. Wang and D. H. Lee, Phys. Rev. B **67**, 020511 (2003).

[34] A. Damascelli, Z. Hussain, and Z.-X. Shen, Rev. Mod. Phys. **75**, 473 (2003).

[35] M. Vojta, Phys. Rev. B **66**, 104505 (2002).

[36] D. Podolsky, E. Demler, K. Damle, and B. I. Halperin, Phys. Rev. B **67**, 094514 (2003).

[37] S. A. Kivelson, I. P. Bindloss, E. Fradkin, V. Oganesyan, J. M. Tranquada, A. Kapitulnik, and C. Howald, Rev. Mod. Phys. **75**, 1201 (2003).

[38] The actual composition is more likely $Bi_{2.1}Sr_{1.9}CaCu_2O_{8+\delta}$.

[39] Ch. Renner and O. Fischer, Phys. Rev. B **51**, 9208 (1995).

[40] S. H. Pan, J. P. O'Neal, R. L. Badzey, C. Chamon, H. Ding, J. R. Engelbrecht, Z. Wang, H. Eisaki, S. Uchida, A. K. Gupta, K. W. Ng, E. W. Hudson, K. M. Lang, and J. C. Davis, Nature (London) **413**, 282 (2001).

[41] H. J. Schulz, Phys. Rev. Lett. **64**, 1445 (1990).

[42] A. Polkovnikov, M. Vojta, and S. Sachdev, Phys. Rev. B **65**, 220509 (2002).

[43] S. M. Hayden, G. H. Lander, J. Zarestky, P. J. Brown, C. Stassis, P. Metcalf, and J. M. Honig, Phys. Rev. Lett. **68**, 1061 (1992).

[44] C. H. Chen, S.-W. Cheong, and A. S. Cooper, Phys. Rev. Lett. **71**, 2461 (1993).

[45] J. M. Tranquada, D. J. Buttrey, V. Sachan, and J. E. Lorenzo, Phys. Rev. Lett. **73**, 1003 (1994).

[46] J. M. Tranquada, J. E. Lorenzo, D. J. Buttrey, and V. Sachan, Phys. Rev. B **52**, 3581 (1995).

[47] P. T. Sprunger, L. Petersen, E. W. Plummer, E. Laegsgaard, and F. Besenbacher, Science **275**, 1764 (1997).

[48] H. Eisaki, N. Kaneko, D. L. Feng, A. Damascelli, P. K. Mang, K. M. Shen, Z. X. Shen, and M. Greven, Phys. Rev. B **69**, 064512 (2004).

[49] H. D. Chen, J. P. Hu, S. Capponi, E. Arrigoni, and S. C. Zhang, Phys. Rev. Lett. **89**, 137004 (2002).

[50] L. Capriotti, D. J. Scalapino, and R. D. Sedgewick, Phys. Rev. B **68**, 014508 (2003).

[51] L. Ozyuzer, J. F. Zasadzinski, K. E. Gray, C. Kendziora, and N. Miyakawa, Europhys. Lett. **58**, 589 (2002).

[52] M. Vershinin, S. Misra, S. Ono, Y. Abe, Y. Ando, and A. Yazdani, Science **303**, 1995 (2004).